ELSEVIER

Regolith history of the aubritic meteorite parent body revealed by neutron capture effects on Sm and Gd isotopes

Hiroshi Hidaka [a,b,*], Shigekazu Yoneda [c], Kurt Marti [d]

[a] *Department of Earth and Planetary Systems Science, Hiroshima University, Higashi-Hiroshima 739-8526, Japan*
[b] *Project Center of Multiple-Isotope Research for Astro- and Geochemical Evolution (MIRAGE), Hiroshima University, Higashi-Hiroshima 739-8526, Japan*
[c] *Department of Science and Engineering, National Science Museum, Tokyo 169-0073, Japan*
[d] *Department of Chemistry and Biochemistry, University of California, San Diego, La Jolla, CA 92093-0317, USA*

Abstract

Enstatite achondrites (aubrites) when compared to other stone meteorites have unusually long cosmic-ray exposure (CRE) ages. We report here the $^{150}Sm/^{149}Sm$ and $^{158}Gd/^{157}Gd$ ratios in six different structural phases, i.e., light and dark (shocked) grains and in matrix materials of Pesyanoe, in three different fragments from Pena Blanca Spring, and in one from Norton County, Shallowater, and Khor Temiki, to investigate the regolith history on the aubrite parent body. The results from phases components of Pesyanoe confirm earlier reported evidence for regolith irradiation of several aubrites. The inferred neutron fluences for six Pesyanoe separates vary between (2.13 and 2.82) $\times 10^{16}$ n cm^{-2}. The fluences also significantly exceed those expected from cosmic-ray irradiation during transit to Earth and approach those observed in the lunar regolith. These observations confirm that the brecciated Pesyanoe meteorite, which contains solar wind (SW) gases only in dark phases, was processed in a regolith and that structural phases were differentially irradiated before compaction. On the other hand, in some aubrites (Mt. Egerton, Shallowater, Pena Blanca Spring, Norton County) neutron capture effects may entirely be due to space irradiation.
© 2006 Elsevier Inc. All rights reserved.

1. Introduction

The relatively frequent occurrence of solar wind (SW) gases in aubrites (Lorenzetti et al., 2003), the discovery of unusual FeO-rich clasts of unknown origin in Pesyanoe (Ivanova et al., 2002; Mathew and Marti, 2003) and of chondritic inclusions in Cumberland Falls (CF) (Mason, 1962) are several reasons to believe that the grains of aubrites had different histories in the regolith of a parent body. Early work on exposure ages (Eberhardt et al., 1965) indicated a cluster of cosmic-ray exposure (CRE) ages near 40 Ma, but such a cluster has been questioned in recent more comprehensive studies (Lorenzetti et al., 2003). The origin of this class of achondrites continues to be of interest

because of the long CRE ages, which are among the longest of stone meteorites (Lorenzetti et al., 2003). The similarities of mineralogical compositions between aubrites and enstatite chondrites suggest a possible relationship between the two classes, but an origin from the same parent body seems not likely (Brett and Keil, 1986; Keil, 1989).

All aubrites except Shallowater are breccias, and six of them, Pesyanoe, Khor Temiki, Bustee, LEW87007, Y-793592 and EET90033, are regolith breccias (Lorenzetti et al., 2003). In particular, Pesyanoe is well known as a gas-rich meteorite that contains solar-type noble gases probably derived from implantation by an ancient solar wind (Marti, 1969). The noble gas abundance patterns suggest regolith processes not unlike those studied in lunar surface materials. Furthermore, distinct components were reported in fragments of the dark phase of the Pesyanoe meteorite. Large variations of $^{21}Ne_c$ between the light and dark phases studied by Müller and Zähringer (1966) are

---

* Corresponding author. Fax: +81 82 424 0735.
E-mail address: hidaka@hiroshima-u.ac.jp (H. Hidaka).

inconsistent with shielding effects during space irradiation and generate discrepancies in CRE ages (Lorenzetti et al., 2003), but may represent a record of preirradiation of the regolith before compaction into the meteorite. Furthermore, Xe and N isotopic data in the dark portion of the Pesyanoe meteorite suggested the possibility of evolutionary processes before compaction of the meteoritic matter (Mathew and Marti, 2003).

Since cosmic-ray irradiation in space and on surfaces of parent objects induce nuclear reactions that produce radioactive as well as stable nuclides, isotopic compositions of some elements evolve significantly in individual meteorites. Therefore, cosmic ray produced isotopic records have given valuable information on the exposure histories of meteorites in space (e.g., Vogt et al., 1990). Thermalized secondary neutrons which arise from the cascade of interactions are slowing down within meteorites and are captured by isotopes with high capture cross-sections such as ^{149}Sm, ^{155}Gd and ^{157}Gd. Therefore, isotopic shifts due to neutron capture by Sm and Gd isotopes are useful tracers for studying the cosmic-ray exposure histories of planetary materials (Eugster et al., 1970a,b; Lugmair and Marti, 1971; Russ et al., 1972; Russ, 1973; Hidaka et al., 1999). In the early 1970s, pioneering work was performed on the Norton County aubrite (Eugster et al., 1970a), on other meteorites (Eugster et al., 1970b), and on lunar samples (Lugmair and Marti, 1971; Russ et al., 1972; Russ, 1973). More recently, a study of aubrites showed some large isotopic shifts in Sm and Gd, corresponding to neutron fluences of (1.2 to 4.0) $\times 10^{16}$ n cm^{-2} (Hidaka et al., 1999). These neutron fluences are not unlike those of lunar surface materials (e.g., (5.16 to 7.49) $\times 10^{16}$ n cm^{-2} for the drill core at Apollo-15 landing site). Differential sensitivities of Sm and Gd isotopes to epithermal and thermal neutrons and the depth dependence of the production rate of thermal neutrons offer the possibility to study the near-surface irradiation history of aubrites on their parent body (Hidaka et al., 1999), but records of regolith processes in components of breccias are not available. Therefore, we studied neutron irradiation records in some aubrites and in separated phases of the Pesyanoe meteorite. This study may also help to decipher the brecciation history and compaction of aubrites.

2. Experimental methods

2.1. Samples

The Pesyanoe meteorite (3.4 kg) is a brecciated aubrite consisting mainly of enstatite (90 vol.%) with plagioclase (7%), diopside (1%) and forsterite (1%). Besides the main mineral components, Pesyanoe has brecciated inclusions of mixed phases of light- and dark-colored fragments, which were chemically characterized and documented for noble gas isotopic composition (Müller and Zähringer, 1966). In the present work, material was separated from two different Pesyanoe samples (P90 and P92) from different but unknown locations. Sample Pesyanoe-90 was

reported to contain solar-type Xe as well as fractionated Ar and Xe components and nitrogen of non-solar origin (Mathew and Marti, 2003). Noble gas isotopic data gave consistent CRE ages of 41.7 and 43.7 Ma for two enstatite crystals of P-92 (Lorenzetti et al., 2003), but about 60 Ma for subsamples of P90 (Lorenzetti et al., 2003; Mathew and Marti, 2003).

Samples of Pesyanoe, P90 and of P92 (originally about 5 g) from unknown locations, are those used for nitrogen, noble gas and radionuclide studies. Subsamples were selected as four distinct structural phases, two brecciated matrix samples (0.107 g for P92,23; 0.213 g for P92,32), handpicked material of the dark phase (0.183 g for P90,31) and two light-colored fragments (0.206 g for P92,29; 0.245 g for P90,30); sample P92,19 of 0.210 g represents a concentrate of white enstatite crystals.

Bulk sample data on neutron capture systematics from only five aubrites were reported (Hidaka et al., 1999). Therefore, additional Sm and Gd isotopic data from other aubrites will provide better statistics regarding regolith histories of aubrites. In the present study, besides the six separates of Pesyanoe, three chips of Pena Blanca Spring (hereafter, PBS), and one each from Norton County (NC), Khor Temiki (KT), and Shallowater (SW) were also measured.

2.2. Analytical procedures

A mass of 0.1–0.2 g of each sample was powdered and decomposed by HF-HClO$_4$. After evaporation to dryness, the sample was re-dissolved in 2 mL of 2 M HCl. The sample solution was loaded onto a first cation exchange packed column (Bio-Rad AG50WX8, 200–400 mesh, H$^+$ form, l 50 mm $\times$ ϕ 4.0 mm), and washed with 4.7 ml of 2 M HCl before REE were eluted with 3 ml of 6 M HCl. Sm and Gd were separated from the other REE through a second ion exchange column (l 100 mm $\times$ ϕ 2.5 mm) packed LN resin (produced from Eichrom Technologies Inc., particle size of 100–150 µm) by elution with 0.35 and 0.5 M HCl, respectively. The total procedural blanks of Sm and Gd were less than 200 pg for each element, which correspond to <0.1% of those in sample. A Micromass VG 54-30 thermal ionization mass spectrometer equipped with seven Faraday cup collectors was used for the isotopic measurements of Sm and Gd. Detailed procedures of the mass spectrometry were previously reported (Hidaka et al., 1995).

3. Results and discussion

Isotopic compositions of Sm and Gd in six samples of Pesyanoe, three of Pena Blanca Spring, one each of Norton County, Khor Temiki, and Shallowater, are summarized in Tables 1(a) and 1(b). The results of Gd in Pesyanoe (P92,32), Khor Temiki, Shallowater and three Pena Blanca Spring samples are not reported in the table because of poor analytical precision due to the weak ion intensities (<1.0 $\times 10^{-12}$ A for ^{158}Gd$^+$) or rapid decay of the ion

Table 1(a)
Isotopic composition of Sm

Sample	$^{148}Sm/^{152}Sm$	$^{149}Sm/^{152}Sm$	$^{150}Sm/^{152}Sm$	$^{154}Sm/^{152}Sm$
STD1	0.420442 ± 5	0.516872 ± 4	0.275980 ± 3	0.850854 ± 7
STD2	0.420450 ± 2	0.516720 ± 2	0.276140 ± 2	0.850825 ± 4
Pesyanoe (P90,29)	0.420456 ± 21	0.516155 ± 27	0.276698 ± 20	0.850881 ± 30
Pesyanoe (P90,30)	0.420452 ± 39	0.516191 ± 30	0.276716 ± 33	0.850839 ± 52
Pesyanoe (P90,31)	0.420446 ± 9	0.516276 ± 11	0.276559 ± 7	0.850822 ± 41
Pesyanoe (P92,32)	0.420476 ± 14	0.516079 ± 11	0.276745 ± 10	0.850913 ± 24
Pesyanoe (P92,23)	0.420442 ± 30	0.516216 ± 28	0.276622 ± 22	0.850883 ± 44
Pesyanoe (P92,19)	0.420493 ± 64	0.516196 ± 75	0.276664 ± 66	0.850887 ± 95
Norton County	0.420443 ± 9	0.516511 ± 10	0.276375 ± 7	0.850872 ± 17
Khor Temiki	0.420446 ± 16	0.516734 ± 15	0.276160 ± 11	0.850841 ± 23
Pena Blanca Spring 1	0.420457 ± 25	0.516843 ± 22	0.276037 ± 16	0.850840 ± 34
Pena Blanca Spring 2	0.420451 ± 22	0.516813 ± 23	0.276071 ± 17	0.850868 ± 37
Pena Blanca Spring 3	0.420446 ± 48	0.516798 ± 42	0.276113 ± 46	0.850886 ± 52
Shallowater	0.420442 ± 18	0.516821 ± 15	0.276000 ± 15	0.850873 ± 22

All standards errors of the last digits indicated are 2σ of the mean.
The data are normalized to $^{147}Sm/^{152}Sm = 0.56081$.
STD1 is a non-irradiated standard material ($\Psi = 0$ n cm^{-2}).
STD2 is a neutron-irradiated standard material ($\Psi = 5.94 \times 10^{15}$ n cm^{-2}).

Table 1(b)
Isotopic composition of Gd

Sample	$^{154}Gd/^{160}Gd$	$^{155}Gd/^{160}Gd$	$^{157}Gd/^{160}Gd$	$^{158}Gd/^{160}Gd$
STD1	0.099747 ± 2	0.676932 ± 5	0.715878 ± 4	1.135846 ± 7
STD2	0.099718 ± 3	0.676767 ± 6	0.715264 ± 5	1.136358 ± 6
Pesyanoe (P90,29)	0.099780 ± 33	0.676598 ± 40	0.713826 ± 29	1.137769 ± 35
Pesyanoe (P90,30)	0.099761 ± 40	0.676197 ± 68	0.713647 ± 52	1.138118 ± 47
Pesyanoe (P90,31)	0.099767 ± 35	0.676251 ± 66	0.713692 ± 57	1.137979 ± 71
Pesyanoe (P92,23)	Not analyzed	0.676290 ± 60	0.713720 ± 39	1.137844 ± 63
Pesyanoe (P92,19)	Not analyzed	0.676252 ± 78	0.713509 ± 81	1.138161 ± 62
Norton County	0.099768 ± 42	0.676494 ± 78	0.714843 ± 78	1.136889 ± 89

All standards errors of the last digits indicated are 2σ of the mean.
The data are normalized to $(^{155}Gd + ^{156}Gd)/^{156}Gd = 1.61290$.
STD1 is a non-irradiated standard material ($\Psi = 0$ n cm^{-2}).
STD2 is a neutron-irradiated standard material ($\Psi = 5.94 \times 10^{15}$ n cm^{-2}).

beam. In order to quantitatively estimate neutron fluences from the isotopic shifts on $^{150}Sm/^{149}Sm$ and $^{158}Gd/^{157}Gd$ in the aubrites, non-irradiated and neutron-irradiated (5.94×10^{15} n cm^{-2}) Sm and Gd chemical reagents were prepared as standard materials STD1 and STD2, respectively (Hidaka et al., 1995) and the isotopic compositions were analyzed. The data of STD1 and STD2 are also compiled in Tables 1(a) and 1(b).

3.1. Estimation of neutron fluences

Isotopic data and inferred neutron fluences of individual samples are reported in Table 2, and Fig. 1 shows the Sm and Gd isotopic correlations. The neutron fluence, Ψ, was calculated from the $^{150}Sm/^{149}Sm$ ratios as follows:

$$\Psi = \frac{(^{150}Sm/^{149}Sm)_{sample} - (^{150}Sm/^{149}Sm)_{STD1}}{(^{150}Sm/^{149}Sm)_{STD2} - (^{150}Sm/^{149}Sm)_{STD1}} \times \frac{\sigma_{STD2}}{\sigma_{sample}}$$
$$\times (0.594 \times 10^{16}),$$

where σ_{sample} and σ_{STD2} are effective neutron capture cross-sections for each sample and for neutron-irradiated standard STD2, respectively. The values of σ_{sample} were calculated by the method of Lingenfelter et al. (1972), and are shown in Table 2.

The ^{149}Sm and ^{157}Gd isotopic depletions in all samples quantitatively correspond to ^{150}Sm and ^{158}Gd enrichments, respectively, documenting the occurrence of neutron capture reactions. The neutron fluences inferred from Sm and Gd isotopic shifts of the six Pesyanoe phases show $\sim30\%$ variations and correspond to fluences in the range from 2.13×10^{16} to 2.82×10^{16} n cm^{-2}. These fluences are higher than those of other aubrites except for Cumberland Falls (CF) (3.99×10^{16} n cm^{-2}) (Hidaka et al., 1999). Furthermore, the inferred fluences of Pesyanoe are about two times higher than those observed in the large (>1100 kg) aubrite Norton County (1.19×10^{16} to 1.48×10^{16} n cm^{-2}). Based on the CRE ages of Pesyanoe (42–63 Ma) and NC (111 Ma) (Lorenzetti et al., 2003), the inferred fluences of

Table 2
Parameters for neutron capture effects

Sample	$^{150}Sm/^{149}Sm$	$^{158}Gd/^{157}Gd$	σ ($\times 10^{-20}$ cm^{-2})	Ψ ($\times 10^{16}$ n cm^{-2})	$\varepsilon_{Sm}/\varepsilon_{Gd}$
STD1	0.533943 ± 7	1.586647 ± 13		0	—
STD2	0.534409 ± 4	1.588725 ± 14	5.0	0.594	
Pesyanoe (P90,29)	0.536075 ± 48	1.593902 ± 81	5.1	2.66 ± 0.08	0.50 ± 0.01
Pesyanoe (P90,30)	0.536073 ± 71	1.594791 ± 133	4.9	2.77 ± 0.10	0.44 ± 0.02
Pesyanoe (P90,31)	0.535681 ± 18	1.594496 ± 161	5.2	2.13 ± 0.05	0.37 ± 0.01
Pesyanoe (P92,32)	0.536245 ± 22	Not reported	5.2	2.82 ± 0.06	Not determined
Pesyanoe (P92,23)	0.535865 ± 52	1.594244 ± 124	5.2	2.36 ± 0.08	0.43 ± 0.01
Pesyanoe (P92,19)	0.535967 ± 150	1.595160 ± 201	5.1	2.53 ± 0.20	0.46 ± 0.01
Norton County	0.535081 ± 17	1.590404 ± 214	4.9	1.48 ± 0.04	0.51 ± 0.03
Khor Temiki	0.534434 ± 26	Not reported	5.0	0.63 ± 0.04	Not determined
Pena Blanca Spring 1	0.534083 ± 38	Not reported	5.0	0.18 ± 0.05	Not determined
Pena Blanca Spring 2	0.534180 ± 41	Not reported	5.0	0.30 ± 0.05	Not determined
Pena Blanca Spring 3	0.534276 ± 99	Not reported	5.0	0.42 ± 0.13	Not determined
Shallowater	0.534034 ± 33	Not reported	5.0	0.12 ± 0.04	Not determined

Analytical errors of $^{150}Sm/^{149}Sm$ and $^{158}Gd/^{157}Gd$ ratios are 2σ of mean. Ψ value was calculated from the following equation:

$$\Psi = \frac{(^{150}Sm/^{149}Sm)_{sample} - (^{150}Sm/^{149}Sm)_{STD1}}{(^{150}Sm/^{149}Sm)_{STD2} - (^{150}Sm/^{149}Sm)_{STD1}} \times \frac{\sigma_{STD2}}{\sigma_{sample}} \times (0.594 \times 10^{16}).$$

$\varepsilon_{Sm}/\varepsilon_{Gd}$ values are the ratios of the ^{149}Sm to ^{157}Gd capture rates defined as

$$\frac{\varepsilon_{Sm}}{\varepsilon_{Gd}} = \frac{\frac{(^{150}Sm/^{149}Sm)_{sample} - (^{150}Sm/^{149}Sm)_{STD}}{1 + (^{150}Sm/^{149}Sm)_{sample}}}{\frac{(^{158}Gd/^{157}Gd)_{sample} - (^{158}Gd/^{157}Gd)_{STD}}{1 + (^{158}Gd/^{157}Gd)_{sample}}}.$$
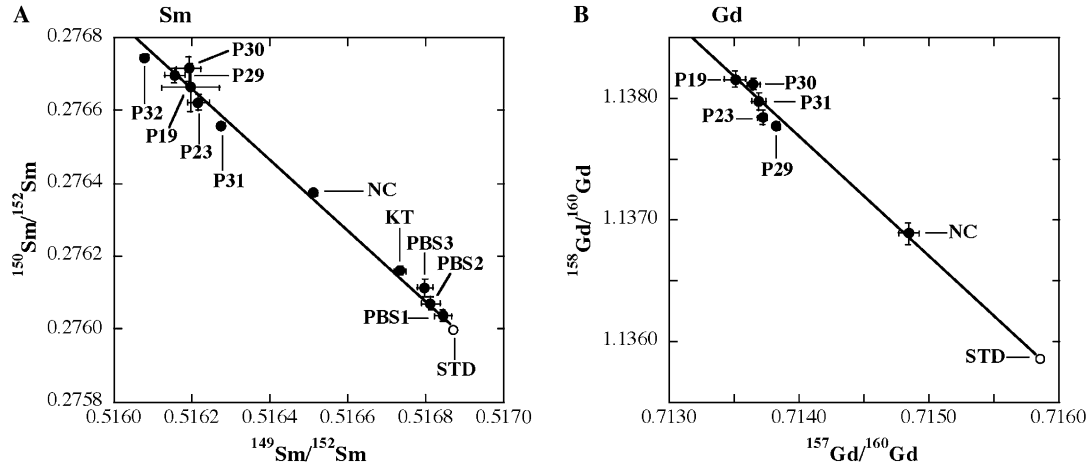

Fig. 1. A correlation diagram of isotopic shifts for (A) $^{149}Sm/^{152}Sm$ vs. $^{150}Sm/^{152}Sm$, and (B) $^{157}Gd/^{160}Gd$ vs. $^{158}Gd/^{160}Gd$ in aubrites. A solid line in each figure shows the ideal neutron capture line.

Pesyanoe exceed those expected from space exposure. In contrast, the neutron fluence calculated for Shallowater, $(1.2 \pm 0.4) \times 10^{15}$ n cm^{-2}, represents the lowest fluence so far determined in aubrites. The neutron flux in a meteorite varies with the shielding depth and chemical composition (Eberhardt et al., 1963; Spergel et al., 1986; Masarik and Reedy, 1994), but the shape of the energy spectra in the range of thermal to epithermal neutrons is insensitive to location of the sample in a meteoroid (Spergel et al., 1986). An extensive study of cosmic-ray tracks indicates that NC samples are confined largely to preatmospheric

depths of 11–21 cm (Bhandari et al., 1980), and this may account for the fact that only 20% differences in neutron fluences were observed between the present and published data (Eugster et al., 1970a,b; Hidaka et al., 1999) in spite of the large recovered mass of NC. On the other hand, observed fluence variations in Pesyanoe subsamples cannot be explained as a depth effect, because the samples were separated from cm-size fragments. We also note that the hand-picked dark material (P90,31) shows the smallest neutron fluence, consistent with previously observed low $^{21}Ne_c$ concentrations in dark material (Lorenzetti et al., 2003).

For a discussion of irradiation records of the Pesyanoe samples, we need to be aware of variations in chemical compositions of the samples. Differences in chemical composition can be treated by the effective total macroscopic neutron capture cross section, $\sum_{\mathrm{eff}}$, on the basis of the conventional calculation obtained mainly from major elements of individual samples (Lingenfelter et al., 1972). $\sum_{\mathrm{eff}}$ characterizes the total neutron absorption for a target material of given chemical composition, and it is defined as the sum over all elements of the products of each element's abundance and its effective cross section. Because the dominant absorbers of neutrons are Fe, Ti and rare earth elements, the $\sum_{\mathrm{eff}}$ values vary with the contents of these elements. As a result, aubrites have rather uniform $\sum_{\mathrm{eff}}$ values (0.0015 to 0.0023 cm^2 g^{-1}) (Hidaka et al., 1999) which are considerably lower than those for chondrites (0.007 to 0.0075) and for lunar materials (0.007 to 0.013). The $\sum_{\mathrm{eff}}$ value of average Pesyanoe determined as 0.0016 g cm^{-2} (data of Lorenzetti et al., 2003) is similar to those of other aubrites. Different structural phases of Pesyanoe have variable $\sum_{\mathrm{eff}}$ values ranging from 0.0014 to 0.0017 g cm^{-2}. However, for equilibrium conditions of the neutron fluences, individual small structured phases have no significant influence on average neutron fluences in the bulk meteorite. The Pesyanoe separates of P90 and P92, respectively, were obtained from cm-size samples and experienced negligible flux differences during space (4π) exposure. The variability in neutron fluences observed in Pesyanoe establishes a regolith evolution and varying histories for components of this breccia.

3.2. Neutron fluences vs. CRE ages

Although large isotopic anomalies in Sm and Gd due to neutron capture were observed in five aubrites, the estimated fluences were not consistent with CRE ages (Hidaka et al., 1999). This suggested multi-step irradiation histories for aubrites, with possible first stage irradiations near the surface of the parent body, and then space (4π) exposure after ejection from the parent body.

The analytical data from the present work permit us now to address in more detail the inferred lack of a correlation between neutron fluences in aubrites and their CRE ages. Fig. 2 illustrates the lack of a correlation of inferred neutron fluences with CRE ages of aubrites (filled circles). For reference we include also data from the literature (filled triangles) (Lugmair and Galer, 1992; Bogard et al., 1995). We can estimate predicted ranges of neutron fluences during 4π exposure for bodies of various sizes and compare these to measured NC data in an attempt to distinguish aubrite histories with and without regolith evolution. As additional supporting data, the ^{10}Be, ^{26}Al and ^{41}Ca concentrations in Norton County place an upper limit on the preatmospheric radius of 50 cm and the depth of the sample from near surface (<5) to 33 cm (Fink et al., 1992, 2002; Welten et al., 2002, 2004). This is supported also by the results of track-density analyses (Bhandari et al., 1980).
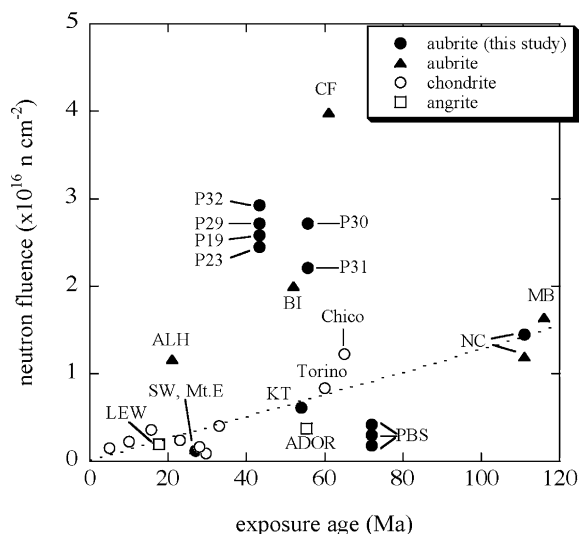

Fig. 2. Comparison of the data between thermal neutron fluences from Sm isotopic shifts and CRE ages from noble gases isotopic analyses. The data of aubrites measured in this study (●: P, Pesyanoe; PBS, Pena Blanca Spring; SW, Shallowater; KT, Khor Temiki; NC, Norton County) are plotted together with other data; aubrites from Hidaka et al. (1999) ▲ (ALH, ALH78113; CF, Cumberland Falls; BI, Bishopville; MB, Mayo Belwa; Mt.E, Mt. Egerton); chondrites from Bogard et al. (1995) and Hidaka et al. (2000a) ○; angrites (ADOR, Angra dos Reis; LEW, LEW86010) from Lugmair and Galer (1992) □. The broken line in the figure was made from upper limits of NC, which suggests the transition region between "no preirradiation" and "with preirradiation" on the parent regolith (see text).

Furthermore, Fink et al. (2002) estimated neutron fluences of (0.3 to 1.3) $\times 10^{16}$ n cm^{-2} for Norton County from their ^{41}Ca data. Thus it is clear by reference to theoretical calculations (Eberhardt et al., 1963; Spergel et al., 1986) and also considering uncertainties in object geometries in space that the neutron flux in aubritic material during its 4π irradiation in space could not have been much greater (less than a factor of two) than 1.5×10^{16} n cm^{-2}, the values from Norton County samples used in this study. Similar arguments were used in the evaluation of space exposure for the aubrites Cumberland Falls, Mayo Belwa, Bishopville and Pesyanoe (Welten et al., 2004). For the purpose of characterizing aubrites with and without regolith evolution, we will take the neutron fluences of 1.48×10^{16} n cm^{-2} for the Norton County sample (Table 2) as approximate limits for the 4π irradiation of aubrites and plot inferred limits for fluences by 4π irradiation in Fig. 2 as a dotted line.

Fig. 2 shows a group of aubrites which apparently had only space irradiation (Shallowater, Pena Blanca Spring, NC), but also a group with evidence for preirradiation in the regoliths (ALH78113, Pesyanoe, Bishopville, Mayo Belwa and CF). Lorenzetti et al. (2003) previously used neutron capture systematics in an attempt to disentangle 2π-parent object-irradiation effects from space exposure in 4π geometry and concluded that neutron fluxes inferred for Cumberland Falls and for Bishopville, based on their CRE ages, would exceed the calculated neutron

production rates ($E < 10$ MeV). The difference in neutron fluences for two NC samples suggests a variation in shielding depth during the 4π irradiation which is supported by measured ^{10}Be and ^{26}Al activities (Fink et al., 2002; Welten et al., 2004) and by track-density systematics (Bhandari et al., 1980) of NC. The dotted line in Fig. 2 represents a visual help for the boundary between "no preirradiation" and "with preirradiation" on the aubrite parent regolith. According to this figure, Khor Temiki may have recorded only space exposure (4π), but this conflicts with the fact that this meteorite contains solar wind gases. Therefore, it must have been at least briefly located in the parent body regolith, and its location (Fig. 2) close to the boundary appears appropriate. However, the approximate boundary line can be improved once different sized aubrites (e.g., NC) which recorded only 4π irradiation are fully documented. Another possible way to separate the cosmic-ray effects due to exposure of meteoroids in space (4π) and those accumulated during regolith exposure (2π) is to use correlations with radionuclide abundances which do not record earlier regolith processes because of short half-lives, if the CRE ages are much longer than the half-lives of the radionuclides. A comparison of observed abundances of ^{10}Be and ^{26}Al with calculated production rates shows that most aubritic meteoroids had small preatmospheric radii less than 60 cm (Welten et al., 2002, 2004).

The concentrations of ^{41}Ca produced from neutron capture in ^{40}Ca in aubrites range from 0.04 to 0.39 dpm/g Ca except for a high value of 2.94 dpm/g Ca for Cumberland Falls (Welten et al., 2004). The inferred neutron fluxes based on ^{41}Ca are much lower than those inferred from the Sm and Gd isotopic shifts and their CRE ages. In the case of Mayo Belwa the evidence implies that one of the longest CRE ages (117 Ma) of stone meteorites (Lorenzetti et al., 2003) is due in part to pre-irradiation in the regolith.

For reference, we also show data for chondrites (open circles) which do show a trend between neutron fluences and CRE ages, although most of the chondrites, except Chico and Torino, have low neutron fluences and short CRE ages. As concerns Torino, a complex exposure history was inferred (Bhandari et al., 1989; Wieler et al., 1996). Although the neutron fluence of Chico is considered to be predominantly produced by a single stage 4π exposure (Bogard et al., 1995), it cannot be used as a possible reference to estimate 4π production of Gd and Sm isotopic shifts, since the chondritic compositions and, therefore, the neutron propagation differ. We note that gas-rich meteorites such as Kapoeta (howardite) and Fayetteville (H chondrite) also reveal relatively high neutron fluences as inferred from observed ^{150}Sm/^{149}Sm isotopic shifts, which suggest that these meteorites also indicate a cosmic-ray irradiation in their parent body regoliths (Rajan and Lugmair, 1988). However, the neutron fluences inferred for Kapoeta and Fayetteville, 2.0×10^{15} and 3.8×10^{15} n cm^{-2}, respectively, are low in comparison to those of aubrites; both also have much shorter CRE ages.

3.3. Neutron energy deduced from $\varepsilon_{Sm}/\varepsilon_{Gd}$

We now address the question of the neutron energy spectrum using the isotopes ^{149}Sm and ^{157}Gd which have different resonance energies for neutron capture at 0.0973 and 0.0314 eV, respectively. The determination of the neutron energy spectrum provides useful information on the sizes of the meteoroids and the depths of the samples during irradiation. Fig. 3 shows a plot for the relation of Sm and Gd isotopic shifts defined as parameter $\varepsilon_{Sm}/\varepsilon_{Gd}$ as a function of composition $\sum_{eff}$. A lower $\varepsilon_{Sm}/\varepsilon_{Gd}$ ratio implies a softer neutron spectrum with more thermalized neutrons, whereas a high value implies a hard spectrum. Inferred effective cross-sections for measured aubrites were reported to be quite constant (Hidaka et al., 1999). In this study, we make more detailed analyses because of chemically heterogeneous compositions observed in aubrites. The calculated effective macroscopic capture cross-sections (Fig. 3) are based on the composition of the studied material (Tables A1 and A2 in Lorenzetti et al., 2003). This presents a difficulty for brecciated aubrites with abundant and large inclusions of apparently chondritic composition and, therefore, may have significantly different neutron slowing-down properties as a result of the presence of alien inclusions. For example, this may be the case for CF, which also reveals a very large neutron capture effect in ^{80}Kr and ^{82}Kr (Lorenzetti et al., 2003), which at least in part may suggest larger Br abundance, as is observed in enstatite chondrites. The calculated neutron energy spectra defined by $\varepsilon_{Sm}/\varepsilon_{Gd}$ ratios as a function of $\sum_{eff}$ (Lingenfelter et al., 1972)
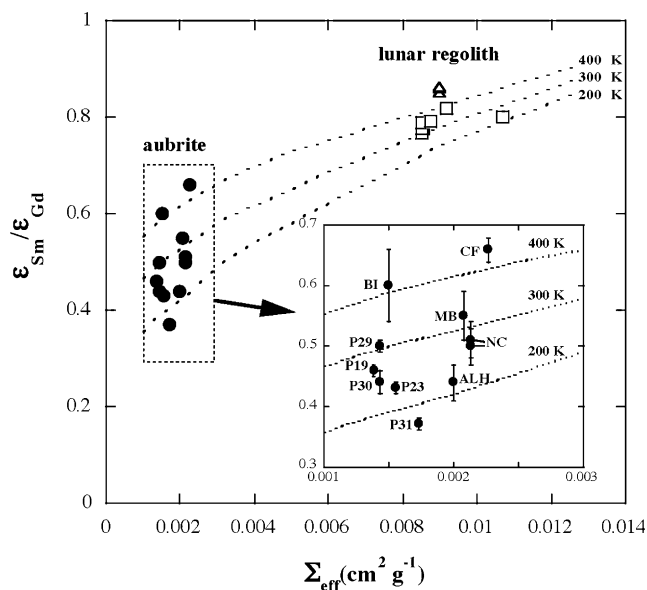

Fig. 3. Neutron energy data of aubrites shown by $\varepsilon_{Sm}/\varepsilon_{Gd}$ vs. $\sum_{eff}$ diagram. The lines in the figure represent predicted neutron energy spectra at three different temperature, 200, 300 and 400 K, estimated from conventional method (Lingenfelter et al., 1972). The data of lunar samples are also plotted in the same figure; A-12 (Hidaka et al., 1999) △; A-15 (Hidaka et al., 2000b) □. The data points of aubrites surrounded with dashed line are enlarged in the right-lower side.

expected at three different temperatures (200, 300 and 400 K) are also given in the figure. All six $\varepsilon_{Sm}/\varepsilon_{Gd}$ ratios of Pesyanoe phases (ranging from 0.37 to 0.50) are lower than those of other aubrites (0.50 to 0.66), even if the slight difference of $\sum_{eff}$ values does affect the variation of neutron energy spectrum. It is significant that variations of $\varepsilon_{Sm}/\varepsilon_{Gd}$ ratios are observed in six Pesyanoe separates (a 3.4 kg meteorite) which document differential neutron irradiation environments in the regolith. The data are consistent with either variation in the effective temperatures of the parent body during irradiation or, more likely, a variation of exposure condition of the various structural elements of the Pesyanoe breccia during parent body irradiation.

Solar noble gases were observed in the dark phase of Pesyanoe (Müller and Zähringer, 1966) and the CRE ages (^{21}Ne ages) based on (^{22}Ne/^{21}Ne)$_c$ ratios and elemental abundances of this sample's dark and light phases are 24.5 and 36.3 Ma, respectively and differ from other CRE ages of Pesyanoe (Lorenzetti et al., 2003). This discrepancy also suggests a differential preirradiation of components in the regolith before compaction of the Pesyanoe meteorite. The $\varepsilon_{Sm}/\varepsilon_{Gd}$ value of our separated material of the dark phase (0.37) is significantly lower than those of five other separates (0.43–0.51), indicating a more thermalized neutron energy spectrum. In support of this, the data from lunar regolith suggest that the neutron spectrum is more thermalized in a deeper layer (around 190 g cm^{-2}) than it is at shallower depth (Hidaka et al., 2000b). However, this then contrasts with the evidence for implanted solar wind gases in the dark phase which requires an exposure in the surface layers at some point in time. These records require that either the surface layer was buried and further irradiated at depth before compaction, or a vertical mixing of components. The variation in $\varepsilon_{Sm}/\varepsilon_{Gd}$ ratios among the Pesyanoe separates favors the latter explanation. The lunar $\varepsilon_{Sm}/\varepsilon_{Gd}$ ratios (Fig. 3) show quite different $\sum_{eff}$ values and, therefore, abundances of neutron absorbing nuclides. From the observed Sm and Gd isotopic shifts in drill core samples of the Apollo-15 landing site, a predicted depth dependence in $\varepsilon_{Sm}/\varepsilon_{Gd}$ ratios has been inferred (Hidaka et al., 2000b). The observed variations in $\varepsilon_{Sm}/\varepsilon_{Gd}$ values in the Pesyanoe samples show that migration of materials can be inferred from documented irradiation conditions. A scenario is required in which different Pesyanoe breccia constituents were irradiated under variable shielding conditions for the individual structural materials before compaction.

4. Conclusions

The observed variations in fluence Ψ and in $\varepsilon_{Sm}/\varepsilon_{Gd}$ values in the Pesyanoe phases show that regolith processes such as vertical migration of materials can be inferred from structural components of a single breccia. A regolith evolution scenario is required in which different breccia constituents were irradiated before compaction under dynamical conditions, permitting a range of fluences, $\varepsilon_{Sm}/\varepsilon_{Gd}$ ratios

and solar wind loading at the surface. Although the space (4π) exposure conditions of the two studied Pesyanoe samples were similar, the inferred CRE-neon ages differ by about 25% (Lorenzetti et al., 2003), while variations in the thermal neutron fluences Ψ (Tables 1(a) and 1(b) and Fig. 2) cover a range of 30%. These systematics show that irradiations in the regolith account for a significant fraction of the total exposure time as implied by CRE ages. We can set an upper limit for space (4π) exposure time for Pesyanoe, based on the Ne data for Pesyanoe (dark) (Müller and Zähringer, 1966), which correspond to $\sim$25 Ma, but this includes the time required for regolith processes such as solar wind loading.

The regolith history on the aubrite parent is of interest also with regard to the parent body size required for regolith evolution. It was suggested that among the asteroids with E-asteroid spectral characteristics probably no large objects exist, since the largest (44 Nysa) has a radius of $\sim$35 km (Chapman et al., 1975). In this case, the irradiation histories documented for Pesyanoe and for other aubrites suggest that regolith evolution may not be limited to larger object. However, it is also possible that the larger and friable parent bodies were fragmented in collisional events. Although there are some similarities with the regolith history for the Moon, the old ages of aubrites imply that the irradiation data characterize processes which took place at different times, presumably early in solar system history.

References

Bhandari, N., Lal, D., Rajan, R.S., Arnold, J.R., Marti, K., Moore, C.B., 1980. Atmospheric ablation in meteorites: a study based on cosmic ray tracks and neon isotopes. *Nucl. Tracks* **4**, 213–262.

Bhandari, N., Bonino, G., Callegari, E., Cini Castagnori, G., Mathew, K.J., Padia, J.T., Queirazza, G., 1989. The Torino, H6, meteorite shower. *Meteoritics* **24**, 29–34.

Bogard, D.D., Nyquist, L.E., Bansal, B.M., Garrison, D.H., Wiesmann, H., Herzog, G.F., Albrecht, A.A., Vogt, S., Klein, J., 1995. Neutron-capture ^{36}Cl, ^{41}Ca, ^{36}Ar, and ^{150}Sm in large chondrites: evidence for high fluences of thermalized neutrons. *J. Geophys. Res.* **100**, 9401–9416.

Brett, R., Keil, K., 1986. Enstatite chondrites and enstatite achondrites (aubrites) were not derived from the same parent body. *Earth Planet. Sci. Lett.* **81**, 1–6.

Chapman, C.R., Morrison, D., Zellner, B., 1975. Surface properties of asteroids: a synthesis of polarimetry, radiometry, and spectrophotometry. *Icarus* **25**, 104–130.

Eberhardt, P., Geiss, J., Lutz, H., 1963. Neutrons in meteorites. In: Geiss, J., Goldberg, E.D. (Eds.), *Earth Science and Meteoritics*. North-Holland, Amsterdam, pp. 143–168.

Eberhardt, P., Eugster, O., Geiss, J., 1965. Radiation ages of aubrites. *J. Geophys. Res.* **70**, 4427–4434.

Eugster, O., Tera, F., Burnett, D.S., Wasserburg, G.J., 1970a. Neutron capture effects in Gd from the Norton County meteorite. *Earth Planet. Sci. Lett.* **7**, 436–440.

Eugster, O., Tera, F., Burnett, D.S., Wasserburg, G.J., 1970b. Isotopic composition of gadolinium and neutron-capture effects in some meteorites. *J. Geophys. Res.* **75**, 2753–2768.

Fink, D., Klein, J., Dezfouly-Arjomandy, B., Middleton, R., Herzog, G.F., Albrecht, A., 1992. ^{41}Ca in the Norton County aubrite. *Lunar & Planet. Sci.* **XXIII**, 355–356.

Fink, D., Ma, P., Herzog, G.F., Albrecht, A., Garrison, D.H., Bogard, D.D., Reedy, R.C., Masarik, J., 2002. ^{10}Be, ^{26}Al, ^{36}Cl, and non-spallogenic ^{36}Ar in the Norton County aubrite. *Meteorit. Planet. Sci.* **37**, A46.

Hidaka, H., Ebihara, M., Shima, M., 1995. Determination of the isotopic compositions of samarium and gadolinium by thermal ionization mass spectrometry. *Anal. Chem.* **67**, 1437–1441.

Hidaka, H., Ebihara, M., Yoneda, S., 1999. High fluences of neutrons determined from Sm and Gd isotopic compositions in aubrites. *Earth Planet. Sci. Lett.* **173**, 41–51.

Hidaka, H., Ebihara, M., Yoneda, S., 2000a. Isotopic study of neutron capture effects on Sm and Gd in chondrites. *Earth Planet. Sci. Lett.* **180**, 29–37.

Hidaka, H., Ebihara, M., Yoneda, S., 2000b. Neutron capture effects on samarium, europium, and gadolinium in Apollo 15 deep drill-core samples. *Meteorit. Planet. Sci.* **35**, 581–589.

Ivanova, M.A., Burbine, T.H., Dickinson, T.L., McCoy, T.J., 2002. An FeO-rich clast from the Pesyanoe aubrite: Indigenous or foreign? *Lunar & Planet. Sci.* **XXXIII**. Abstract #1080.

Keil, K., 1989. Enstatite meteorites and their parent bodies. *Meteoritics* **24**, 195–208.

Lingenfelter, R.E., Canfield, E.H., Hampel, V.E., 1972. The lunar neutron flux revisited. *Earth Planet. Sci. Lett.* **16**, 355–369.

Lorenzetti, S., Eugster, O., Busemann, H., Marti, K., Burbine, T.H., McCoy, T.J., 2003. History and origin of aubrites. *Geochim. Cosmochim. Acta* **67**, 557–571.

Lugmair, G.W., Marti, K., 1971. Neutron capture effects in lunar gadolinium and the irradiation histories of some lunar rocks. *Earth Planet. Sci. Lett.* **13**, 32–42.

Lugmair, G.W., Galer, S.J.G., 1992. Age and isotopic relationships among the angrites Lewis Cliff 86010 and Angra dos Reis. *Geochim. Cosmochim. Acta* **56**, 1673–1694.

Marti, K., 1969. Solar-type xenon: a new isotopic composition of xenon in the Pesyanoe meteorite. *Science* **166**, 1263–1265.

Masarik, J., Reedy, R.C., 1994. Effects of bulk composition on nuclide production processes in meteorites. *Geochim. Cosmochim. Acta* **58**, 5307–5317.

Mason, B., 1962. *Meteorites*. John Wiley and Sons Inc., New York.

Mathew, K.J., Marti, K., 2003. Solar wind and other gases in the regoliths of the Pesyanoe parent object and the moon. *Meteorit. Planet. Sci.* **38**, 627–643.

Müller, O., Zähringer, J., 1966. Chemische unterschiede bei uredelgashaltigen steinmeteoriten. *Earth Planet. Sci. Lett.* **1**, 25–29.

Rajan, R.S., Lugmair, G.W., 1988. Solar flare tracks and neutron capture effects in gas-rich meteorites. *Lunar Planet. Sci.* **XIX**, 964–965.

Russ, G.P., 1973. Apollo 16 neutron stratigraphy. *Earth Planet. Sci. Lett.* **17**, 275–289.

Russ, G.P., Burnett, D.S., Wasserburg, G.J., 1972. Lunar neutron stratigraphy. *Earth Planet. Sci. Lett.* **15**, 172–186.

Spergel, M.S., Reedy, R.C., Lazareth, O.W., Levy, P.W., Slatest, L.A., 1986. Cosmogenic neutron-capture-produced nuclides in stony meteorites. *J. Geophys. Res.* **91**, D483–D494.

Vogt, S., Herzog, G.F., Reedy, R.C., 1990. Cosmogenic nuclides in extraterrestrial materials. *Rev. Geophys.* **28**, 253–275.

Welten, K.C., Nishiizumi, K., Caffee, M.W., 2002. Cosmogenic radionuclides in aubrites. *Lunar & Planet. Sci.* **XXXIII**. Abstract #2043.

Welten, K.C., Nishiizumi, K., Hillegonds, D.J., Caffee, M.W., Masarik, J., 2004. Unraveling the exposure histories of aubrites. *Meteorit. Planet. Sci.* **39**, A113.

Wieler, R., Graf, T., Signer, P., Vogt, S., Herzog, G.F., Tuniz, C., Fink, D., Fifield, L.K., Klein, J., Middleton, R., Jull, A.J.T., Pellas, P., Masarik, J., Dreibus, G., 1996. Exposure history of the Torino meteorite. *Meteorit. Planet. Sci.* **31**, 265–272.